Journal of Sound and Vibration (1999) **221**(3), 371–389
Article No. jsvi.1998.1976, available online at http://www.idealibrary.com on IDEAL

DYNAMIC RESPONSE OF A STIFFENED LAMINATED COMPOSITE PLATE SUBJECTED TO BLAST LOAD

H. S. Türkmen and Z. Mecitoğlu

Istanbul Technical University, *Aeronautics and Astronautics Faculty*, *Maslak*, *Istanbul* 80626, *Turkey*

(*Received* 20 *April* 1998, *and in final form* 22 *September* 1998)

This paper is concerned with the experimental and numerical study of stiffened laminated composite plates exposed to a normal blast shock wave. For this purpose a detonation is developed from the reaction of LPG–O_2 mixtures in a long circular cylindrical shock tube. The detonation wave goes through into the atmosphere from the open end of the shock tube and acts as a blast load on the stiffened laminated composite plate which is placed in front of the detonation tube. Mounting of the target plate on a steel frame is designed with the object of providing clamped boundary conditions. The air blast pressure distribution is obtained by the use of quartz crystal pressure transducers placed on the wooden model. Strains are measured at the different points on the stiffened laminated composite plate and stiffener. In the experiment and analysis two different load cases are examined. Furthermore, a finite element modelling and analysis of the blast loaded stiffened composite plate are presented and the numerical results are compared with the experimental ones. An agreement is found between the experimental and finite element results in both linear and non-linear ranges. A good prediction is performed for the peak strain in the plate. However a discrepancy is shown between the measured and predicted strains on the stiffener because of the adhesive layer between the plate and stiffener. Prediction of the response frequency that has a great importance in the dynamic phenomena correlates well with the experimental results. The effects of stiffener and loading conditions on the dynamic behavior are examined. Large deformation effects are taken into account for the second loading condition.

1. INTRODUCTION

The dynamic response of structures to air blast has for many years been the subject of numerous studies. Most of them are related to the dynamic response of isotropic plate and shell structures subjected to blast load [1–8]. With the advent of new composite material structures and their increased use in the aerospace industry, there is a need to reconsider the problem of structural response. This is due to the fact that new composite material structures exhibit distinguishing features as compared to their metallic counterparts. Composite material structures are

0022–460X/99/130371 + 19 $30.00/0

characterized by a weak rigidity in transverse shear and by high degrees of orthotropy of the layer materials. The difficulties that arise from the complexity of the problem, which involves time-dependent finite deformations, high strain rates and non-linear inelastic material behavior, have motivated various assumptions and approximations to simplify the models. These models span the full range of sophistication from simple one-degree-of-freedom representations to general purpose finite element programs such as NASTRAN, ANSYS, ADINA, etc.

There are studies related to composite material structures subjected to blast load in the literature. Reddy [9] conducted research for the forced motions of laminated composite plates using a finite element that accounts for the transverse shear strains, rotary inertia and large rotations. Nosier *et al*. [10] analyzed the dynamic response of viscously damped laminated composite rectangular flat panels to time-dependent external excitation in the frame of higher order plate theory. They incorporated viscous structural damping and outlined its influence in their study. Numerical results are compared with ones derived within the framework of the first order shear deformation and classical theories and some conclusions concerning their range of applicability are outlined. It was found that the most significant amplitude attenuation due to the damping effect occurred during the free motion range as a general conclusion. Librescu and Nosier [11], in their theoretical analysis of symmetrically laminated rectangular composite flat panels exposed to blast load, took into account transverse shear deformation, transverse normal stress and higher order effects. Recently, a theoretical and numerical study of the dynamic response of a single laminated composite plate subjected to blast load was presented by Türkmen and Mecıtoğlu [12]. These researchers took into account large deformation effects. Türkmen *et al*. [13] investigated the dynamic response of laminated composite panels subjected to blast load theoretically. They compared the theoretical results with numerical ones obtained using the ANSYS finite element software. Furthermore, Türkmen and Mecıtoğlu [14] investigated the dynamic response of laminated composite shells subjected to blast load experimentally and numerically. Türkmen and Mecıtoğlu [15], in their theoretical analysis of laminated composite plates subjected to blast load, took into account geometrical nonlinearities. Türkmen [16] obtained theoretical results for composite plate structures subjected to blast load and compared these results with experimental ones. In his theoretical analysis, transverse shear strains and in-plane inertia were ignored. Experimental studies related to stiffened laminated composite plates subjected to blast load have not been found in the literature.

The area of investigation which specifically concerns this paper is the experimental and numerical study of stiffened laminated composite plates exposed to a normal blast shock wave. On the experimental side of the study, tests have been carried out on stiffened laminated composite plates with clamped edges for various blast loads. A blast load is obtained from the detonation wave which is developed in a tube by the reaction of LPG and oxygen mixtures. On the numerical side of the study, the ANSYS finite element software is utilized for obtaining strain–time histories. Numerical results are compared with experimental ones and

an agreement is found. The effects of the stiffener and loading conditions on the dynamic behavior are examined.

2. EXPERIMENTAL WORK

Experiments are carried out to test stiffened laminated composite plates with clamped edges. A blast loading is obtained from the detonation wave which is developed in a tube by the reaction of LPG and oxygen mixtures. The detonation tube, the stiffened laminated composite plate and the plate mounting frame used in the tests are shown in Figure 1. The detonation tube is fixed to two steel box beams which are clamped to a concrete base seated on the ground. The plate mounting frame is placed in front of the detonation tube. The target plate is mounted between the two steel frames with twelve screws to provide clamped boundary conditions. The plate was positioned on a special plate mounting system shown in Figure 2 which was designed to give fully clamped boundary conditions.

2.1. BLAST PRESSURE MEASUREMENT

The LPG and oxygen mixture is ignited in the detonation tube to obtain an air blast pressure load to subject the plate to. The ratio of LPG and oxygen mixture and the mass of the mixture are stabilized using a computer. The air blast pressure distribution is obtained by quartz crystal pressure transducers placed on a wooden model which was exposed to the blast load. The blast load is applied toward the center of plate. Assuming the distribution of the blast load on the target plate is symmetrical, the transducers are placed at six points on a quarter of the model (Figure 3). The signal obtained from the transducer is amplified by using a charge

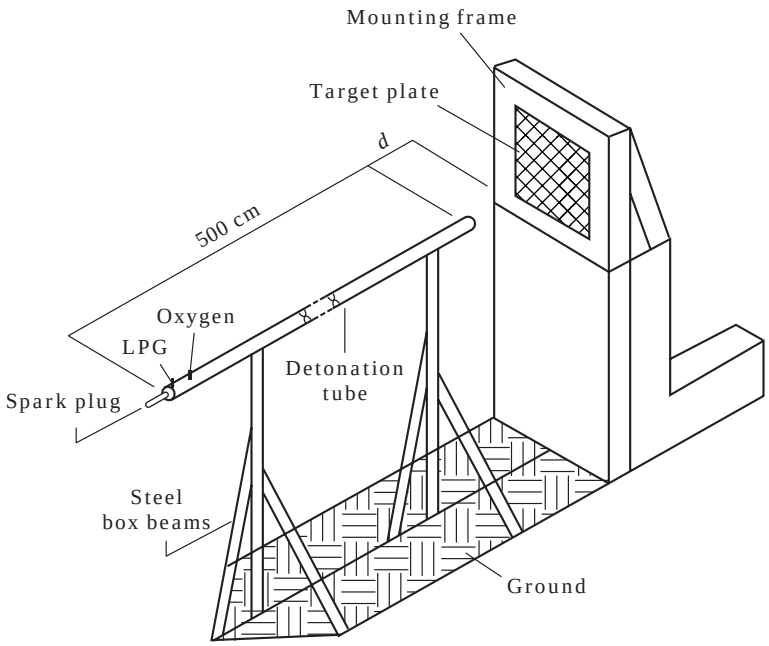

Figure 1. Placement of detonation tube, plate mounting frame and plate.

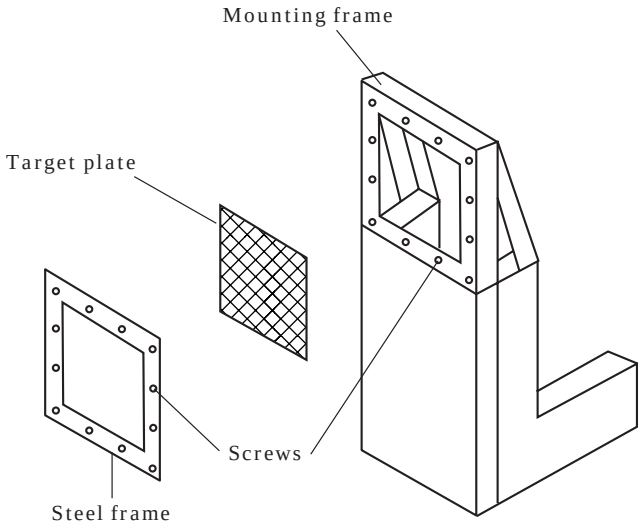

Figure 2. Exploded view of plate mounting system.

amplifier. The air blast pressure distribution is obtained for 100 and 35 cm distances from the detonation tube in this way.

2.2. STRAIN MEASUREMENT

The material of the panels used in the tests is a carbon fiber fabric. Strain-gauges and Wheatstone bridge are used to measure dynamic strains. Two strain-gauges are placed on the back surface of the plate and stiffener to obtain the strain-time history. One strain-gauge is mounted at the D2 point of the plate in the x and y directions (Figure 4). Another strain-gauge is mounted at the D1 point of the stiffener. The original obtained from the bridge circuit is amplified by using a dynamic strainmeter.

The signals obtained from the charge amplifier and the dynamic strainmeter are digitized by using a 100 MHz digital scope and the data are transferred to a PC

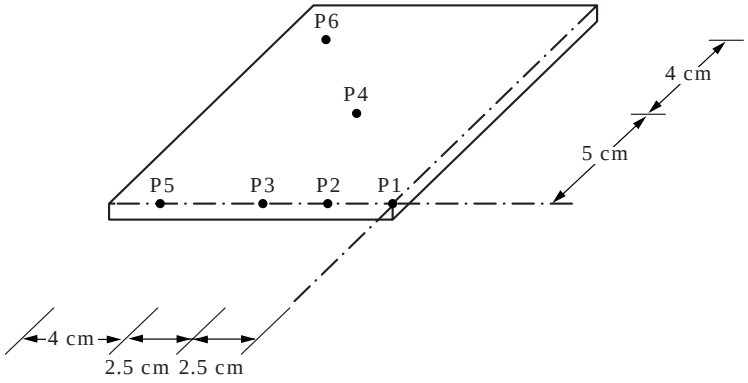

Figure 3. Placement of the pressure transducers.

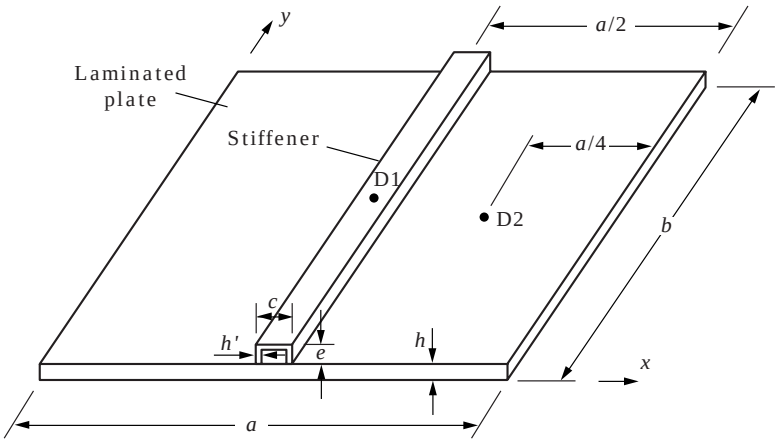

Figure 4. Placement of the strain–gauges.

computer by using a RS232C serial interface. All processes to develop the detonation wave and measurements of pressure and strain on the stiffened plate are controlled using a PCL818 card and a PC computer. The experimental setup is shown in Figure 5.

3. FINITE ELEMENT ANALYSIS

The laminated plate and Cartesian co-ordinate system are depicted in Figure 4. In this study, the ANSYS5.3 finite element software is used in the modelling and analysis of the stiffened plate. The finite element model for the stiffened laminated composite plate consists of an assembly of 2-D shell elements with five layers in the transverse direction (Figure 6). The stiffener is modelled using 2-D shell elements with three layers in the transverse direction. The plate and stiffener are discretized by the use of eight-nodded laminated shell elements named SHELL91. The geometry, node locations, and the co-ordinate system for this element are shown in Figure 7 [17]. The element has six degrees of freedom at each node: translations in the nodal x, y and z directions and rotations about the nodal x, y and z axes. SHELL91 may be used for layered applications of a structural shell model or for modelling thick sandwich structures. Up to 16 different layers are permitted for applications with the sandwich option turned off. In the finite element model, no slippage is assumed between the element layers. Shear deflections are included in the element, however; normals to the center plane before deformation are assumed to remain straight after deformation. The stress varies linearly through the thickness of each layer [18].

Three different models which consisted of uniform grids with 24, 48 and 88 shell elements were used to verify the accuracy of the finite element model of the plate. Modal analysis is performed to obtain the natural frequencies of the plate. Comparison of the natural frequencies for the first ten modes shows considerable differences when changing the grid mesh from 24 to 48 elements, and small differences when refining this grid from 48 to 88 elements. Convergency of the

fundamental frequency shows that the mesh of 88 elements is sufficient to give adequate accuracy. Therefore the plate and stiffener are modelled using 88 and 32 laminated shell elements, respectively.

The transient dynamic analysis technique was used to obtain the strain time history at the points D1 and D2 of the stiffened plate. These analyses were carried out using two different loading conditions. In the first, the pressure is uniformly distributed on the plate. Small deformations are considered for the finite element analysis of the plate under this first loading condition. In the second, a non-uniform pressure distribution is assumed on the plate, and geometric non-linearities are included in the analysis. The pressure load which is obtained from experiments is applied on the whole surface of the plate as a function of the

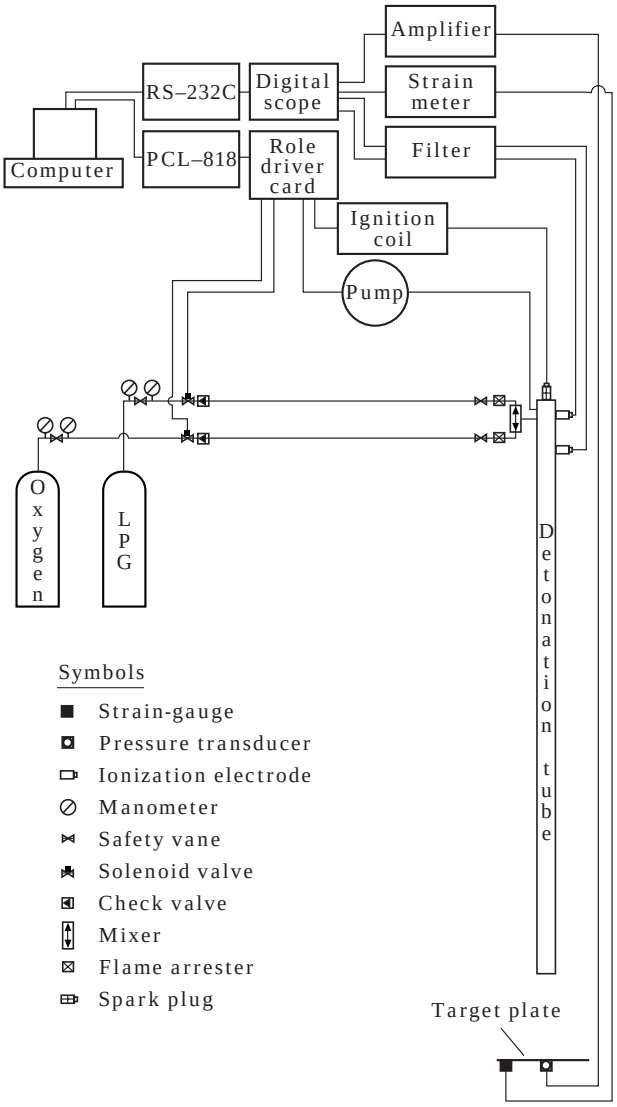

Figure 5. Experimental set-up.

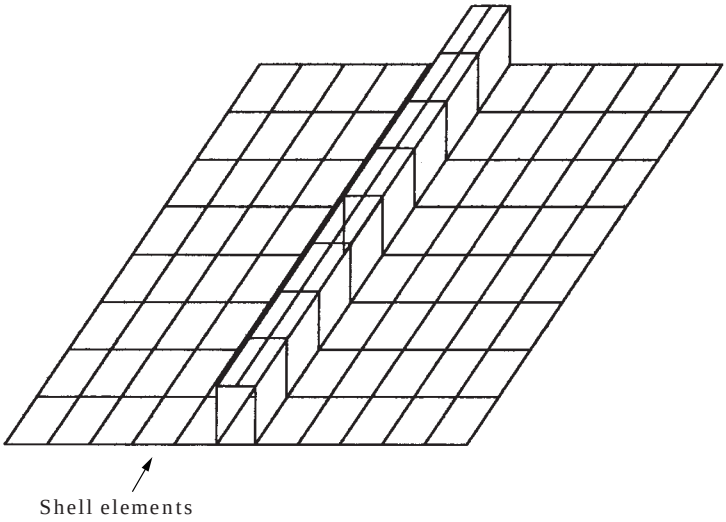

Figure 6. Finite element model.

time. For this purpose the modified Friedlander decay function [3] is used in the analysis. This function is expressed as

$$p(t) = p_m(1 - t/t_p)\,\mathrm{e}^{\alpha t/t_p}. \tag{1}$$

The variation of pressure with time is shown in the Figure 8.

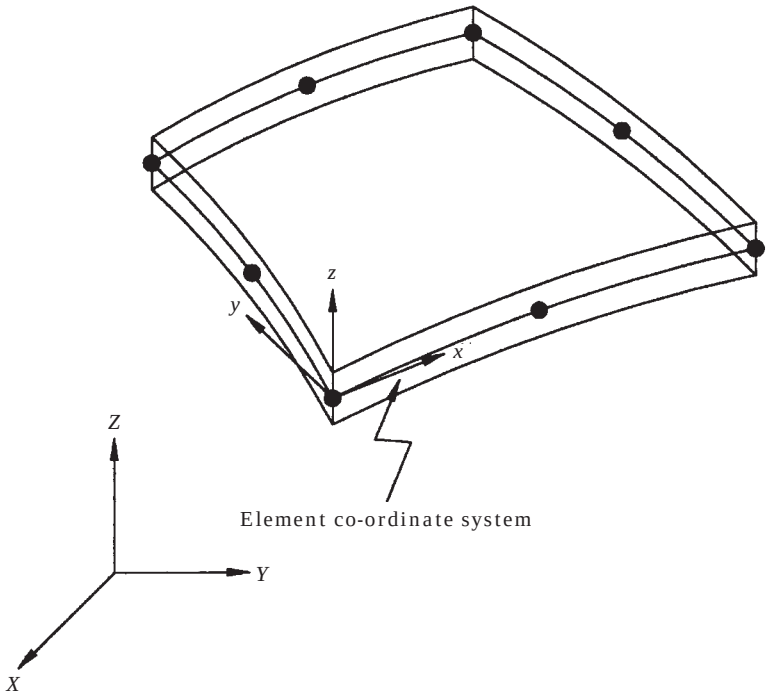

Figure 7. The geometry, node locations, and co-ordinate system.

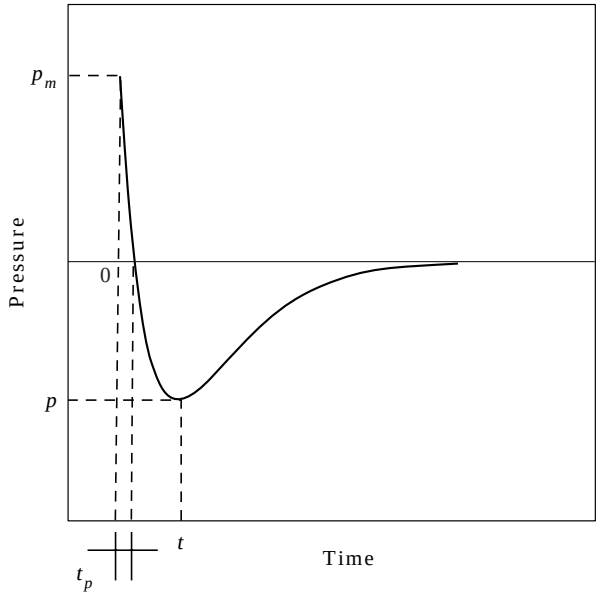

Figure 8. Blast pressure curve.

A total of 40 time function points are used in describing the exponentially decaying blast load for the both analyses. All edges of the plate are modelled by clamped boundary conditions. For the linear transient analysis of the plate, time integration is carried out using the Newmark method [19]. On the other hand, the Newton–Raphson technique is used for the geometrically nonlinear transient analysis [19]. The time increment is taken to be 0·1 ms in both analyses.

4. RESULTS AND DISCUSSION

In this study, the blast loading is obtained from the detonation wave which is developed in a tube by the reaction of LPG and oxygen mixtures. Then, the detonation wave goes through to atmosphere from the open end of the tube and applies a normal blast load on the target plate that is mounted at a distance from the open end of the tube.

Two different distances are experienced: 100 and 35 cm. Pressure transducers are mounted on a wooden model and blast pressure variation and distribution are obtained on the wooden model. Because the plate is symmetrically placed with respect to the axis of shock tube, only a quarter wooden model is used to obtain air blast pressure distribution. The blast pressure is measured at six different points on the quarter model. The blast measurements are repeated three times and average values are calculated.

Pressure measurement results are shown in Tables 1 and 2 for the 100 and 35 cm, respectively. Differences in the distance affect the air blast pressure variation and distribution on the plate. Uniformly distributed air blast pressure is obtained for 100 cm distance from the open end of the tube. The spatial distribution of the peak pressure on the plate is shown in Figure 9 for the 35 cm distance. The pressure–time

TABLE 1

Blast test results (*bar*)

Transducer	Test 1	Test 2	Test 3	P_{av}
1	0·287	0·290	0·289	0·289
2	0·286	0·302	0·285	0·291
3	0·289	0·277	0·311	0·292
4	0·267	0·285	0·298	0·283
5	0·312	0·288	0·322	0·307
6	0·254	0·297	0·295	0·282

TABLE 2

Blast test results (*bar*)

Transducer	Test 1	Test 2	Test 3	P_{av}
1	3·047	2·578	3·281	2·968
2	2·344	2·262	2·237	2·281
3	1·406	1·406	1·406	1·406
4	0·938	0·938	0·911	0·929
5	0·938	0·859	0·937	0·911
6	0·703	1·016	0·703	0·807

variations obtained from the transducer at the point P1 are shown in Figures 10 and 11 for the 100 and 35 cm distances, respectively. The air blast pressure magnitude and variation are afffected by the distance from the open end of the tube. The ratio of the positive peak pressure to the negative peak pressure increases with the increasing distance. In the low distance case, experimental results show that the blast load has a large negative peak pressure since the high portion of the blast pressure is reflected. The blast pressure variation measured in the tests show that the load suddenly increases and then exponentially decays with time.

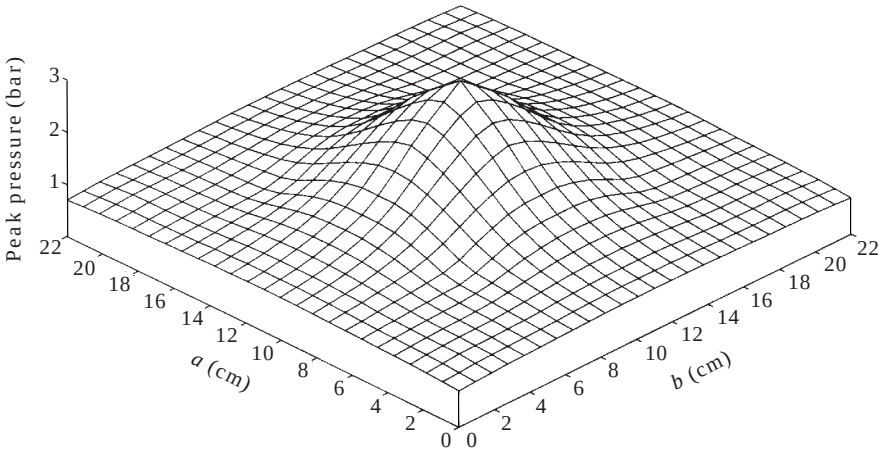

Figure 9. Blast pressure distribution on the plate.

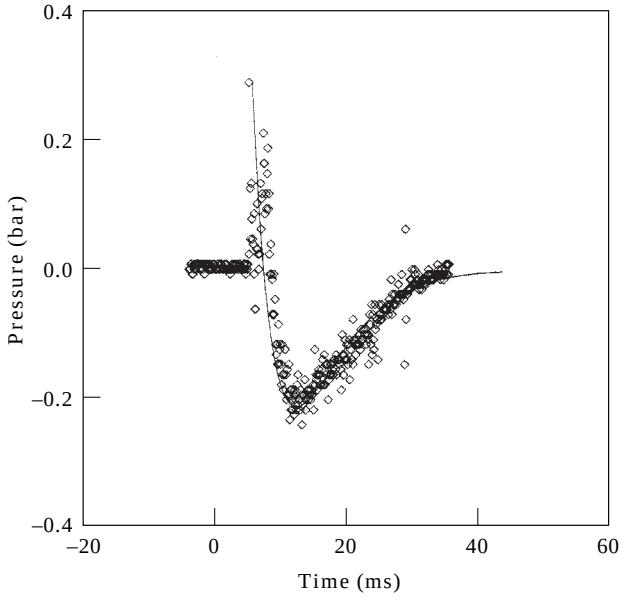

Figure 10. Variation of blast loading by time ($d = 100$ cm). ——, Approximation; ◇, experimental.

During the decaying of blast pressure, some pressure fluctuations are observed because of the dynamic behavior of blast pressure.

An acceptable approximation to the blast loading test results can be accomplished by choosing the appropriate values of the p_m and t_p in equation (1), and then by calculating the waveform parameter α, in terms of them. In this study the values of p_m and t_p are chosen at negative peak pressure time (Figure 8) and

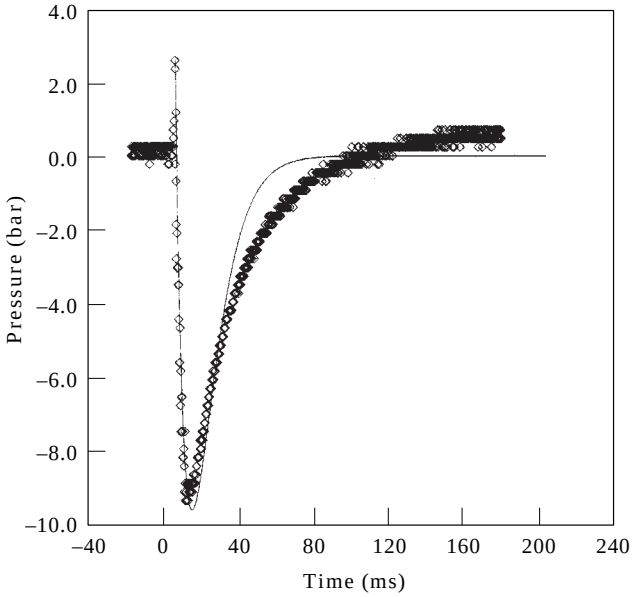

Figure 11. Variation of blast loading by time ($d = 35$ cm). Key as Figure 10.

TABLE 3

Loading conditions

Parameters	Load case I	Load case II
p_m (N/m^2)	28 906	296 875
p_c (N/m^2)	0	70 000
d (cm)	100	35
α	0·35	0·06
t_p (s)	0·0018	0·0009
Pressure distribution	Uniform	Non-uniform

then the waveform parameter is determined. Figures 10 and 11 show the approximate curves for the time variation of the pressure measured at the point P1. In the second loading condition, the pressure time variations obtained from transducers show differences from each other. However, an average pressure time variation is used in the analysis. In the low distance case, the peak pressure values obtained from experiments are applied to the each element, separately.

In the experiments and analysis carbon fiber fabric ply material is used. All layers are taken to be of equal thicknesses. The lay-up used for the specimens is made by hand lay-up technique. Carbon fibers are laid onto a mold by hand and the resin is brushed on. The deposited layers are densified with rollers. Curing is done at room temperature. Strain-gauges and Wheatstone bridge are used to obtain dynamic strain.

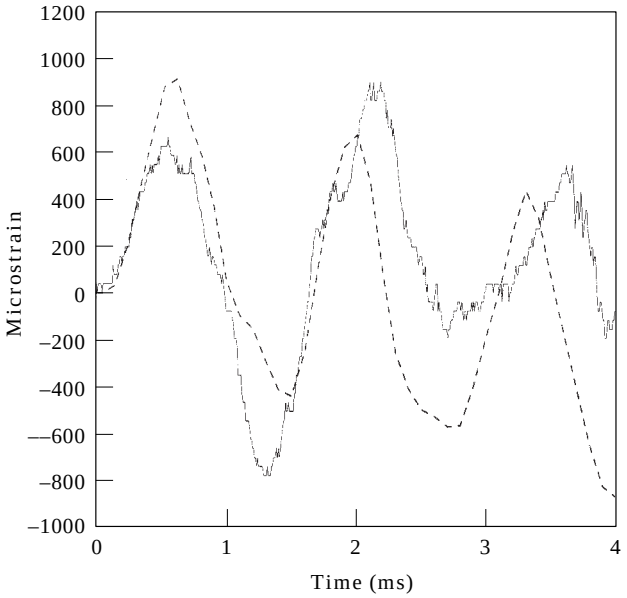

Figure 12. Strain–time history plots in the x-direction at point D2 for first loading condition. ——, Experimental; – – –, ANSYS.

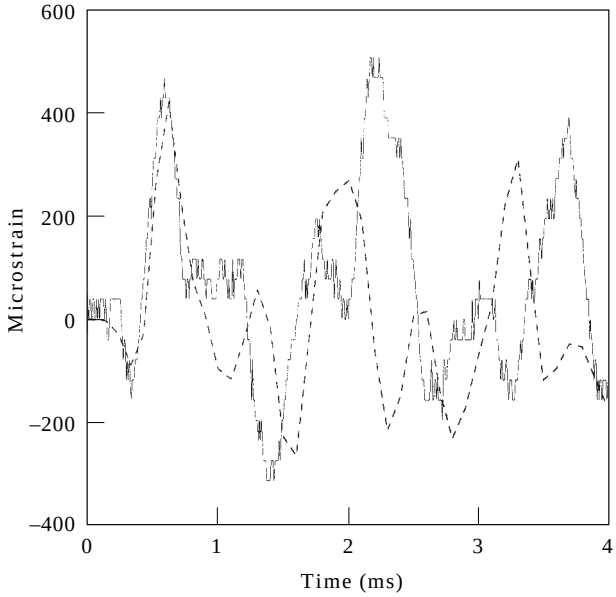

Figure 13. Strain–time history plots in the y-direction at point D2 for first loading condition. Key as Figure 12.

In the numerical analysis the following values of the material and geometrical properties are used: $E_1 = 59{\cdot}32$ GPa, $E_2 = 59{\cdot}32$ GPa, $G_{12} = 3{\cdot}86$ GPa, $v_{12} = 0{\cdot}06$, $\rho = 1430$ kg/m^3, $h_k = 0{\cdot}35$ mm, $a = 22$ cm, $b = 22$ cm, $c = 2$ cm, $e = 1{\cdot}6$ cm, $h = 1{\cdot}75$ mm, $h' = 1{\cdot}05$ mm.

The tests and analyses are performed for the two different loading conditions shown in Table 3. The strain–time history plots for the first loading condition are shown in Figures 12–14. The strain–time histories of the strains in the x and y direction at the point D2 of the plate are shown in Figures 12 and 13, respectively. The strain–time history in the y direction at the point D1 of the stiffener is shown in Figure 14.

The results obtained from the finite element analysis are compared with the experimental results. It is shown that there is a qualitative agreement between them. A good prediction is performed for obtaining peak strains of the point D2 on the plate (Figures 12 and 13). After a short time, the numerical analysis results show differences from experimental results, since the damping effects are ignored in the analysis. The pressure variation obtained from blast tests show that a discrepancy from the approximated curve at the second millisecond after then peak pressure time (Figure 10). Therefore, in Figures 12–14, experimental results show that a discrepancy from the numerical results after the second millisecond. A discrepancy occurs between the prediction and experimental results of the peak strain in the stiffener. This situation can be due to ignoring the effect of adhesive between the plate and stiffener in the analysis. Furthermore the dynamic response frequencies obtained from the finite element method and experimental method are in an agreement.

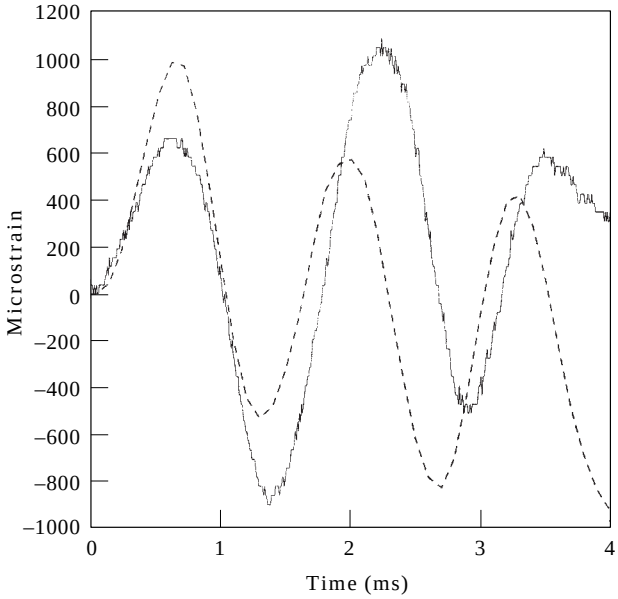

Figure 14. Strain–time history plots in the y-direction at point D1 for first loading condition. Key as Figure 12.

The strain–time history plots for the second loading condition are shown in Figures 15–17. The peak pressure in the case of the second loading condition is approximately ten times of the peak pressure in the case of the first loading condition. However, because of the geometric non-linearities and non-uniform

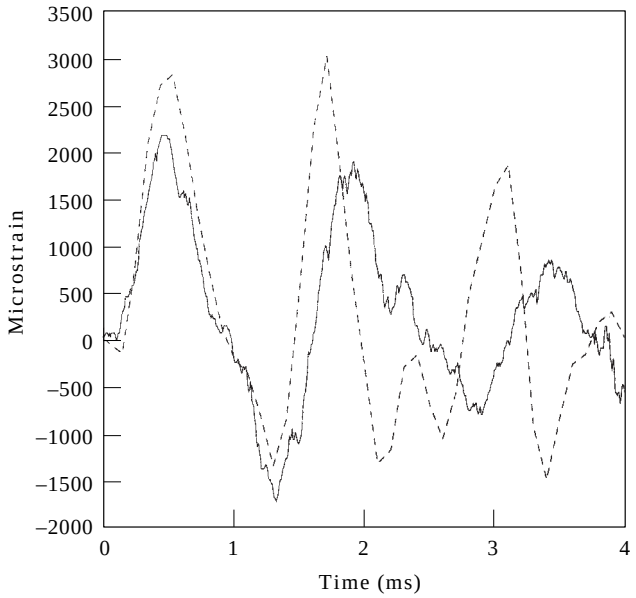

Figure 15. Strain–time history plots in the x-direction at point D2 for second loading condition. Key as Figure 12.

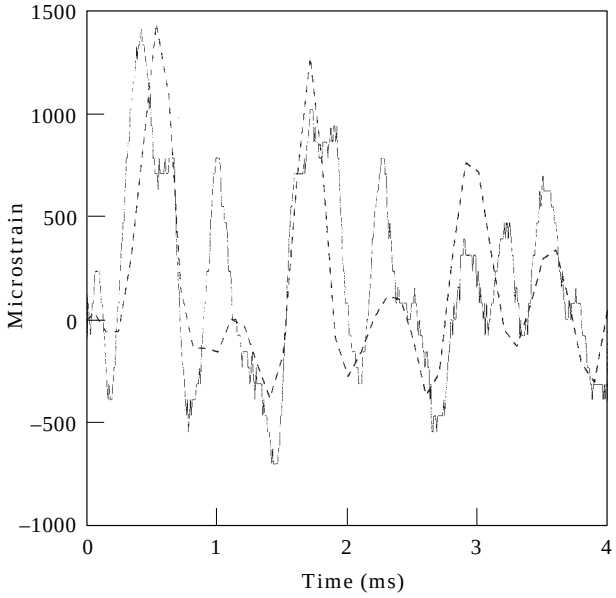

Figure 16. Strain–time history plots in the y-direction at point D2 for second loading condition. Key as Figure 12.

pressure distribution, the strain values in the case of the second loading condition is approximately three times the strain values of the first loading condition. Furthermore, since the plate moves rapidly due to the blast load with high velocity in the second loading condition, the structural damping becomes a more significant factor in restricting the plate response. Therefore the discrepancy between the

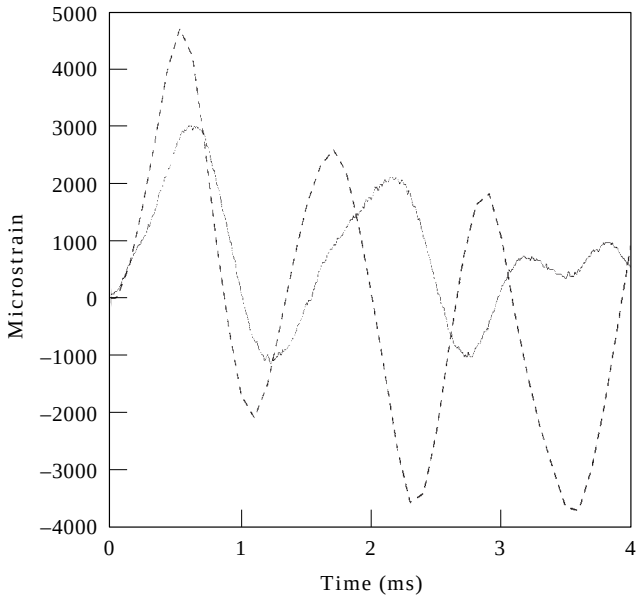

Figure 17. Strain–time history plots in the y-direction at point D1 for second loading condition. Key as Figure 12.

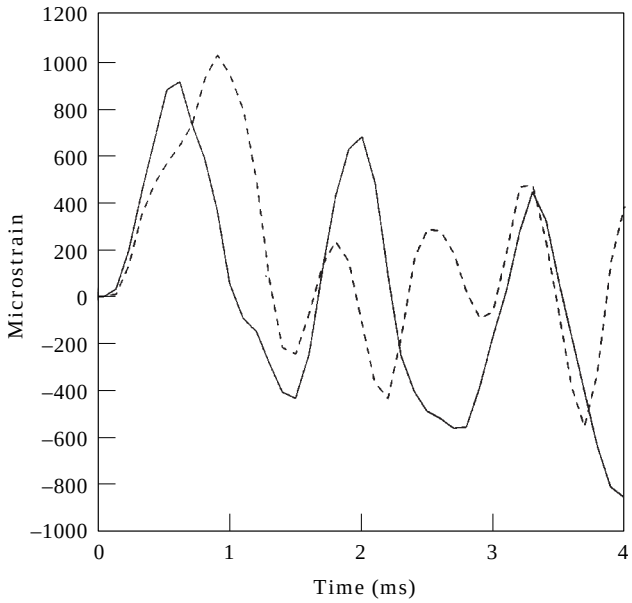

Figure 18. Comparison of the strain–time history in the x-direction at point D2 under first loading condition. ——, stiffened; – – –, unstiffened.

experimental and numerical results is clearer for the case of the second loading condition. A discrepancy occurs between the prediction and experimental results of the peak strain in the stiffener because of the effect of adhesive between the plate and stiffener (Figure 17). Despite the variation of blast loading with time obtained from the blast tests which show differences amongst the different transducer

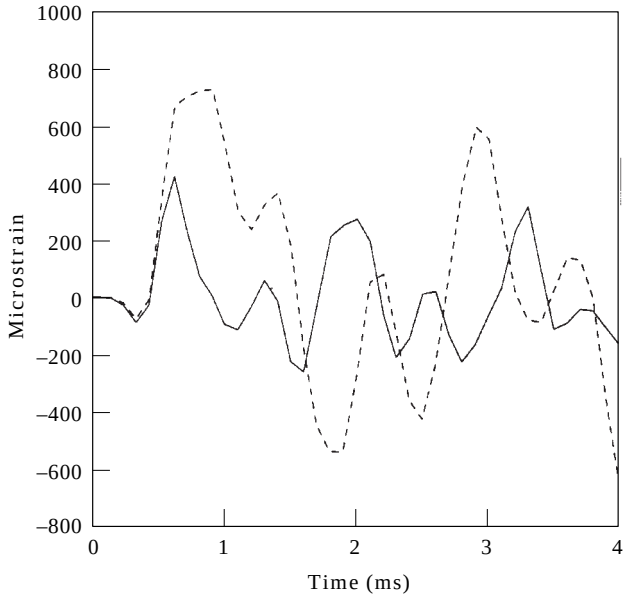

Figure 19. Comparison of the strain–time history in the y-direction at point D2 under first loading condition. Key as Figure 12.

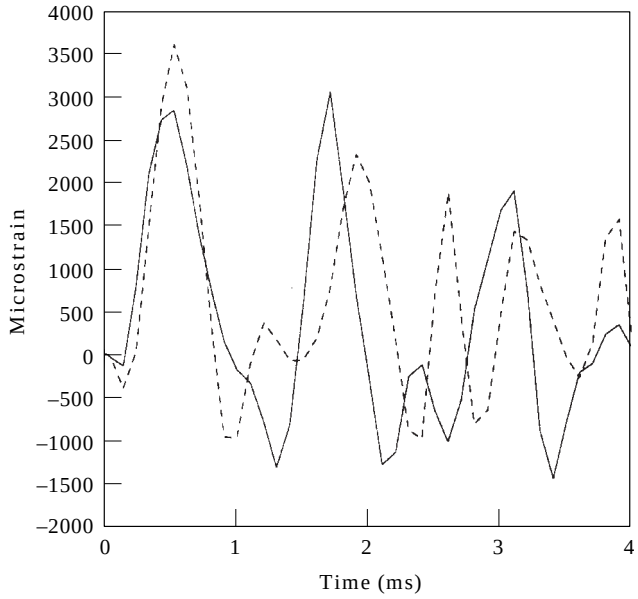

Figure 20. Comparison of the strain–time history in the x-direction at point D2 under second loading condition. Key as Figure 12.

points, an average pressure time variation is used in the analysis. Therefore the additional discrepancy between the experimental and finite element results occurs in the second loading condition. The response frequency agreement between the numerical and experimental results is also obtained in the second loading condition.

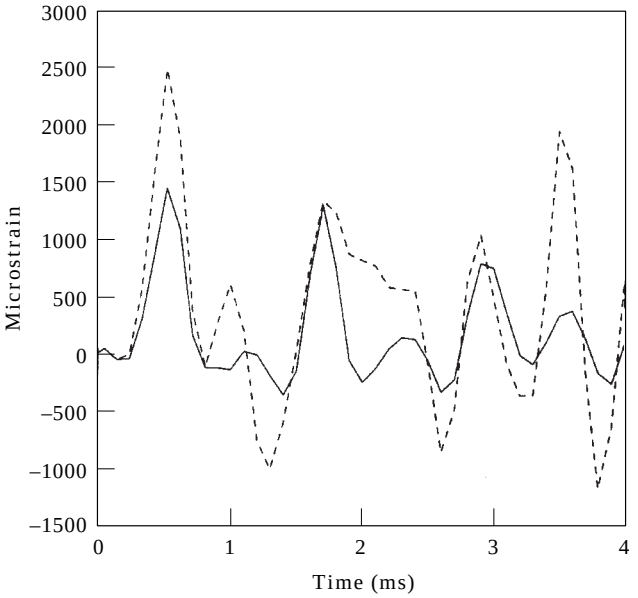

Figure 21. Comparison of the strain–time history in the y-direction at point D2 under second loading condition. Key as Figure 12.

Furthermore the strain–time history results of the stiffened and unstiffened plate, which has the same dimensions as the stiffened plate, subjected to blast load are compared in Figures 18–21. The stiffener reduces the peak strains at point D2 11% and 42% under the first loading condition in the x and y directions, respectively. Under the second loading condition, the stiffener reduces the peak strains at point D2 21% and 42% in the x and y directions, respectively. The effect of the stiffening on the strain in the x-direction is small since the stiffener is bonded in the y direction. The strain–time history results in the x-direction are shown in Figures 18 and 20. Furthermore the strain–time history results are obtained at point D2 instead of at the center of the plate where the biggest effect of stiffening on the dynamic response is seen. Therefore the effect of the stiffening on the dynamic response is found to be small in Figures 18–21.

5. CONCLUSIONS

This paper presents a numerical analysis and correlation with experimental results of the strain–time histories of stiffened laminated composite plates exposed to normal blast shock waves. In the numerical study, finite element modelling and analysis are performed by using ANSYS software. The strain–time history is obtained in both linear and non-linear ranges. The blast wave is assumed to be exponentially decaying with time and either uniformly distributed or non-uniformly distributed on the plate surface. In the experimental study, the air blast pressure distribution is obtained by the use of the quartz crystal pressure transducers placed on a wooden model. Strains are measured at the different points on the stiffened laminated composite plate and stiffener. The following conclusions apply to the case of stiffened laminated plates with clamped boundary conditions as considered herein.

The blast pressure measurements on the plate show that the character of the pressure variation is strongly dependent on the distance from the open end of the tube to the target plate. For example, if we decrease this distance about three times, the peak pressure on the plate increases ten times approximately. Furthermore, the ratio of the positive peak pressure to the negative peak pressure increases with the increasing distance. The blast pressure has a non-uniform distribution on the plate for the case of low distance. On the other hand, the spatial variation of the pressure becomes more uniform as the distance increases.

From the time–response curves, the experimental and numerical results are in good agreement. Then, experimental results show a difference from the numerical results because of the structural damping. The discrepancy between the experimental results and numerical ones is more clear for the low distance case. Because, in this case, the plate moves rapidly due to the blast load with high velocity, and therefore the structural damping becomes more significant factor restricting the plate response. On the other hand, if the frequencies are considered, a good agreement is found between the experimental and numerical results. Although the peak strain depends on the peak pressure value, the variation of the strain with time depends on the pressure time variation. However, a good prediction is performed in both linear and non-linear ranges by using approximate

blast pressure–time variation in the finite element analysis. The adhesive used bonding the plate and stiffener significantly decreases the peak strain value on the stiffener.

The effect of fiber orientation on the dynamic response of the laminated composite plate can be examined by this method. The structural damping and hygro-thermal effects may be interesting in the aspect of the dynamic response of plate. The cutout effects on the dynamic behavior of the plate can be studied by the use of this method. These will be the topics of the next studies.

ACKNOWLEDGMENT

This study was supported in part by a grant from the Istanbul Technical University Research Fund and Turkish Airlines.

REFERENCES

1. R. Houlston, J. E. Slater, N. Pegg and C. G. Desrochers 1985 *Computers and Structures* **21**, 273–289. On analysis of structural response of ship panels subjected to air blast loading.
2. R. Houlston and C. G. Desrochers 1987 *Computers and Structures* **26**, 1–15. Nonlinear structural response of ship panels subjected to air blast loading.
3. A. D. Gupta, F. H. Gregory, R. L. Bitting and S. Bhattacharya 1987 *Computers and Structures* **26**, 339–344. Dynamic analysis of an explosively loaded hinged rectangular plate.
4. J. Jiang and M. D. Olson 1991 *Computers and Structures* **41**, 41–52. Nonlinear dynamic analysis of blast loaded cylindrical shell structures.
5. M. D. Olson 1991 *Computers and Structures* **40**, 1139–1149. Efficient modeling of blast loaded stiffened plate and cylindrical shell structures.
6. D. Redekop and P. Azar 1991 *Journal of Vibration and Acoustics* **113**, 273–278. Dynamic response of a cylindrical shell panel to explosive loading.
7. D. Redekop 1994 *Computers and Structures* **51**, 126–133. Dynamic response of a toroidal shell panel.
8. C. J. Wiernicki, F. Liem, G. D. Woods and A. J. Furio 1990 *Naval Engineers Journal* 192–203. Structural analysis methods for lightweight metallic corrugated core sandwich panels subjected to blast loads.
9. J. N. Reddy 1983 *American Institute of Aeronautics and Astronautics Journal* **21**, 621–629. Geometrically nonlinear transient analysis of laminated composite panels.
10. A. Nosier, L. Librescu and D. Frederick 1990 *Studies in Applied Mechanics* 24, *Advances in the Theory of Plates and Shells*, G. Z. Voyiadjis and D. Karamanlidis, editors. Amsterdam: Elsevier, 249–268. The effects of time-dependent excitation on the oscillatory motion of viscously damped laminated composite flat panels.
11. L. Librescu and A. Nosier 1990 *American Institute of Aeronautics and Astronautics Journal* **28**, 345–352. Response of laminated composite flat panels to sonic boom and explosive blast loadings.
12. H. S. Türkmen and Z. Mecitoğlu 1995 *First International Aerospace and Advanced Technologies Symposium*, 475–484. Dynamic behavior of laminated composite plate subjected to shock loading.
13. H. S. Türkmen, Z. Mecitoğlu and O. Borat 1996 *Mathematical and Computational Applications* **1**, 126–133. Nonlinear structural response of laminated composite panels subjected to blast loadings.
14. H. S. Türkmen and Z. Mecitoğlu 1997 *International Symposium on Aviation*. Dynamic response of a laminated composite shell under blast load.

15. H. S. TÜRKMEN and Z. MECİTOĞLU 1998 Submitted to *American Institute of Aeronautics and Astronautics Journal*. Nonlinear structural response of laminated composite plates subjected to blast loadings.
16. H. S. TÜRKMEN 1998 *Ph.D. thesis*, *Istanbul Technical University*. Dynamic response of laminated composite panels subjected to blast loading.
17. *ANSYS*5.3 *Elements Reference*, 000655, eighth edition, SAS IP, Inc., Chap. 4, 625–636, 1996.
18. *ANSYS*5.3 *Theory Reference*, 000656, seventh edition, SAS IP, Inc., Chap. 14, 344–350, 1996.
19. *ANSYS User's Manual*, *Volume I*, *Procedures*, 000447, Upd0, ANSYS Revision 5.2, SAS IP, Chap. 3 59–92, 1995.